# Creation of photo-modulated multi-state and multi-scale molecular assemblies *via* binary-state molecular switch†

**Yiyang Lin,[a] Xinhao Cheng,[a] Yan Qiao,[a] Cailan Yu,[b] Zhibo Li,[c] Yun Yan[a] and Jianbin Huang*[a]**

***Received 13th August 2009, Accepted 26th November 2009***
***First published as an Advance Article on the web 14th January 2010***
**DOI: 10.1039/b916721h**

The creation of photo-modulated multi-state and multi-scale molecular self-assemblies was realized by the ingenuous utilization of a binary-state molecular switch, sodium (4-phenylazo-phenoxy)-acetate (AzoNa). Depending on the irradiation time, the binary state of the azobenzene group (*i.e. trans*/*cis* isomerization) can be exploited to generate multi-state nanostructures (including wormlike micelle, vesicle, lamellar structure, small micelle) by the coupling of conventional surfactant CTAB. Meanwhile, the conformation transition of azobenzene at molecular scale (~Å), stimulated by light input can be amplified to regulate molecular architectures at mesoscopic scale (from nanometer to micrometer), leading to significant changes in solution property at macroscopic scale (naked-eye visible scale). By exposing to UV or visible light, the multi-state and multi-scale molecular self-assemblies can be reversibly controlled. It is proposed that light-triggered structural changes in the dipole moment and geometry of azobenzene group, which impart a significant effect upon molecular packing of surfactant aggregates, were responsible for this peculiar phenomenon.

## Introduction

Nature has the unique power to assemble molecules in an elegant and efficient manner of multiple weak noncovalent interactions (including hydrogen bond, salt bridges, hydrophobic effect, electrostatic interaction, and metal–ligand coordination), to fabricate sophisticated structures. Inspired by the complexity and diversity of molecular architectures in nature, chemists are facing the problem of how to manipulate molecules in order to construct artificial structures of similar perfection and functionality.[1] The external input that can be exploited to control molecular assembly involves pH,[2] light,[3] temperature,[4] electric,[5] redox,[6] ultrasound,[7] salinity,[8] *etc.*

Among these external stimuli, light is expected to be more advantageous and of significant importance. First, vision and other light-triggered biochemical transformations, such as phototomovement at various biological levels, photomorphogenesis, and conversion of light energy into chemical energy in plants, represent sophisticated biological processes in which optical signals are recorded and transduced as physicochemical events.[9] Second, in contrast to redox regent, pH change, salinity and stress, light signal can be operated in a clean environment free of any additional reagent. Third, light input is the most reliable strategy to tailor molecular assembly in view of its ready availability as a mild energy source.[10] Also, another advantage of light over electric or ultrasound is that, light can be directed at a precise spatial location; this becomes especially valuable in nanoscience and nanotechnology applications, such as sensor systems, nanoelectronics, microfluidic, information storage and MEMS devices.[11]

Therefore, light is considered as an ideal external trigger signal to manipulate molecular assemblies at different hierarchical levels. The research interest involves host–guest chemistry, surfactant self-assembly, molecular machines, surface chemistry, controlled drug release, *etc.* For example, Sakai has controlled the formation and disruption of vesicles by light input in aqueous mixtures of a azobenzene-modified cationic surfactant and an anionic surfactant.[12] Whitten has described the supramolecular aggregates of a series of azobenzene-contained phospholipids and related compounds in bilayer assemblies and other microheterogeneous media.[13] Raghavan and coworkers provided a new class of photorheological fluids that undergo wormlike micelles to short cylindrical micelles transition.[14] Eastoe has utilized UV light to change the ordering in lyotropic lamellar (L$\alpha$) phases.[15]

Despite the number of studies dedicated to investigations of photo-modulated molecular assemblies, there are still open questions remained to be addressed. In most cases, the light signal was translated into discrete "On" and "Off" states of molecular or supramolecular assemblies in a giving system such as photo-mediated aggregation/disaggregation processes, hydrophobic/hydrophilic surface, sol–gel transition, random coil/$\alpha$-helix transitions, capture/release of guest molecules, and organized nanostructures with two distinct morphologies. This mainly originates from the fact that, light-active compounds usually exhibit two states such as trans/cis isomerization in azobenzene, open/close form in diarylethene, monomer/dimer transition in thymine. On the other hand, in these reports, light

[a]*Beijing National Laboratory for Molecular Sciences (BNLMS), College of Chemistry and Molecular Engineering, Peking University, Beijing, 100871, China. E-mail: jbhuang@pku.edu.cn; Fax: +86-10-62751708; Tel: +86-10-62753557*
[b]*CAS Key Laboratory of Photochemistry, Institute of Chemistry, Chinese Academy of Sciences, Beijing, 100080, People's Republic of China*
[c]*State Key Laboratory of Polymer Physics and Chemistry, Institute of Chemistry, Chinese Academy of Sciences, Beijing, 100190, PR China*
† Electronic supplementary information (ESI) available: Synthesis of the azobenzene derivative. See DOI: 10.1039/b916721h

 

was mainly utilized to control molecular self-assembly in the microscopic scale. Nevertheless, the ultimate object of modern chemistry is to manipulate or assemble molecules into complex molecular architectures with morphological diversity at every level.

Stimulated by the curiosity in this field, we are interested in the creation of light-modulated multi-scale and multi-state molecular self-assemblies. In this paper, the peculiar light-active self-assembled system, consisting of azobenzene derivative and conventional surfactant, can exhibit four distinct states depending on illumination time. Combined with the result of transmission electronic microscopy (TEM), rheology, polarizing optical microscopy (POM), dynamic light scattering (DLS), small angle X-ray scattering (SAXS) and macroscopic appearance, we have demonstrated that diverse molecular self-assemblies including small micelle, wormlike micelle, global vesicle, and lamellar structures can be regulated by UV light, accompanied by the variation of solution properties, *e.g.* rheology, flowing birefringence, and phase separation. Moreover, both microstructures and solution properties can be reverted by further stimulation of visible light.

## Experiments and materials

### Materials

Cetyltrimethylammonium bromide (CTAB) was recrystallized five times from acetone. The purity of the surfactant was examined and no surface tension minimum was found in the surface tension curve. 4-hydroxyl azobenzene was bought from Alfa Aesar. The synthesis of sodium (4-phenylazo-phenoxy)-acetate (AzoNa) is described in the Supporting Information (ESI).† Other reagents of AR grade were from Beijing Chemical Co. The water used was redistilled from potassium permanganate containing deionized water to remove traces of organic compounds.

### Sample preparation

The CTAB solution was prepared by dissolving the surfactant solid directly in the test tube. To this solution, a desired amount of AzoNa was added and heated until totally soluble. After stirring for several minutes, the sample was thermostated at 30 °C to reach equilibrium.

### Photoisomeric experiments

For light-triggered *trans*/*cis* transition, solution samples were irradiated with 365 nm UV light from a Spectroline FC-100F fan-cooled, long wave UV lamp. The power of the mercury arc lamp was 100 W. Samples (5 mL) were placed in a quartz tube, and irradiation was applied for a specific duration under stirring. For *cis*/*trans* transition, irradiation by visible light was performed using a 200-W incandescent light bulb (>440 nm).

### Solubility investigation

The solubility of AzoNa isomers in water at 30 °C was determined as follows: an excess amount of AzoNa compound was added to deionized water, and the solution was heated and stirred for 2 h, followed by equilibration at 30 °C for 12 h. The resulting solution was filtered through a 0.20-μm membrane filter of hydrophilic PVDF in order to remove the unresolved precipitate. The UV-vis absorbance was measured and converted to the concentration value determined from a calibration curve.

### Absorbance measurements

The UV-vis absorbance measurements of solution were carried out on the spectrophotometer (Cary 1E, Varian Australia PTY Ltd.) equipped with a thermostated cell holder. The UV-vis measurements were all carried out at 30 °C.

### Transmission electron microscopy

Fracturing and replication were carried out in a freeze-fracture apparatus (BalzersBAF400, Germany) at −140 °C; Pt/C was deposited at an angle of 45° to shadow the replicas, and C was deposited at an angle of 90° to consolidate the replicas; the resulting replicas were examined in a JEM-100CX electron microscope. TEM micrographs were obtained with a JEM-100CX II transmission electron microscope (working voltage of 80–100 kV).

### Cryo-TEM

A small drop of sample was placed on a copper grid, and a thin film was produced by blotting off the redundant liquid with filter paper. This thin film was then quickly dipped into liquid ethane, which was cooled by liquid nitrogen. Observation of the cryo-sample was carried out at −183 °C.

### Rheology measurements

The rheological properties of the samples were measured at 30 °C with a ThermoHaake RS300 rheometer (cone and plate geometry of 35 mm in diameter with the cone gap equal to 0.105 mm). A solvent trap was used to avoid water evaporation. Dynamic oscillation experiments were obtained in the linear viscoelastic regime of each sample as determined by dynamic stress-sweep experiments. For measurements with the light-illuminated surfactant solution, the sample was loaded in near-dark conditions, and the rheometer was covered to prevent conversion to the *trans*-form by ambient light.

### Polarization optical microscopy

The photographs of birefringence in surfactant solution were taken by a polarization microscope (OLYMPUSBH-2).

### Small angle X-ray scattering

Small Angle X-ray Scattering was performed by SAXSess (Anton-Paar, Austria, CuK$\alpha$, $\lambda = 0.154$ nm) in situ, in which the sample was sealed in quartz capillary tubes.

### NMR spectroscopy

NMR measurements were performed on a Bruker NMR spectrometer (resonance frequency of 400 MHz for 1H) operating in the Fourier transform mode. For NMR measurements, samples were prepared in $D_2O$.

### Dynamic light scattering

To prepare dust-free solutions for light scattering measurements, the solutions were filtered through a 0.20-μm membrane filter of hydrophilic PVDF into light scattering cells before the measurements. The light scattering cells had been rinsed with distilled acetone to ensure a dust-free condition before use. DLS was performed with a spectrometer (ALV-5000/E/WIN Multiple Tau Digital Correlator) and a Spectra-Physics 2017 200 mW Ar laser (514.5 nm wavelength). The scattering angle was 90°, and the intensity autocorrelation functions were analyzed by using the methods of Contin.

### Fluorescence measurement

Steady-state fluorescence spectra were obtained with an Edinburgh FLS920 fluorescence spectrophotometer. In these studies, a fixed amount (5.0 μM) of the fluorescent probe Nile Red was added into surfactant solution. The excited wavelength of Nile Red was 575 nm and the emission intensity was monitored.

## Result and discussion

### Photo-triggered *tran*/*cis* isomerization of AzoNa

The anionic azobenzene derivative AzoNa, which may undergo *trans*/*cis* transition as triggered by UV light, was synthesized (Fig. 1a). Before UV illumination, there is about 89% *trans*-content in the solution as calculated from $^1$H NMR spectrum of aromatic protons in azobenzene group (Fig. 1b). After UV illumination, the aromatic protons of the *cis*-azobenzene shift further upfield than those of the *trans*-azobenzene due to the magnetically anisotropic effect (Fig. 1c). The amount of *trans* content was reduced to 8% while the *cis* content can increase to 92% after UV illumination.

The *trans*/*cis* transition can be further evidenced by UV-vis spectra (Fig. 2a). Before irradiation, the spectrum is dominated by the 344 nm absorption which is ascribed to π–π* absorption band of the *trans*-azobenzene moiety. As UV irradiation proceeds, the 344 nm absorption band decreases with concomitant increase of the π–π* and n–π* bands of the *cis* isomer at around 290 nm and 460 nm, respectively. A photostationary state was attained within 30 min. When the irradiated solution was then exposed to visible light, the *trans*-azobenzene can be reverted to *cis*-azobenzene. The *trans*/*cis* isomerization of the azobenzene unit in AzoNa could be repeated many times without decomposition of the components (Fig. 2b). Therefore it is anticipated that AzoNa can be developed as a binary-state molecular switch for constructing photo-modulated molecular assemblies.

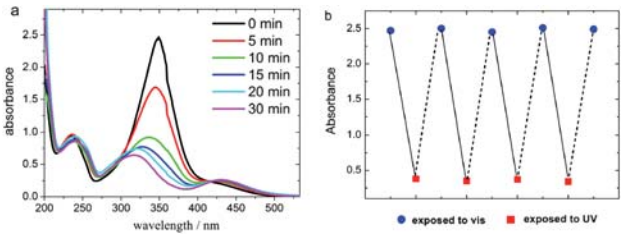


**Fig. 2** (a) UV-vis absorption spectra of AzoNa solution (0.1 mM) at different time of UV irradiation; (b) the absorbance at 344 nm of AzoNa solution by alternate irradiation at UV and visible light, respectively.

### Photo-regulated multi-state and multi-scale molecular self-assemblies

Usually, light-active systems are mainly consisting of single component, which results in molecular self-assemblies lacking in diversity and complexity. Dual-component or multi-component self-assemblies built on multiple weak interactions, however, are expected to open up a multitude of new chances. An outstanding example is the mixture of cationic-anionic surfactants system ("catanionic" mixed surfactant system), which offers an attractive approach for constructing complex self-assembled nanostructures including globular micelles, cylindrical micelles, long threadlike micelle, vesicle, discs, and large lamellar sheets.[16] Inspired by this consideration, we have designed a photo-active pseudo cationic-anionic surfactant system, in which the binary-state molecular switch AzoNa (anionic component) was coupled to the conventional cationic surfactant CTAB. Interestingly, the self-assembled system of 30 mM CTAB and 50 mM AzoNa can undergo four distinct states as a function of UV irradiation time (Fig. 3). As UV illumination time increases, the sample can experience viscoelastic solution with flowing birefringence (wormlike micelle), biphasic solution (coexist of vesicle and lamellar structure), viscoelastic solution without flowing birefringence (wormlike micelle) and water-like solution (small micelle). In this section, the self-assembled molecular architectures and phase behavior will be investigated combined with multiple techniques.

Before UV illumination (donated as *state one*), the sample was equilibrated under visible light to generate a transparent, gel-like appearance (Fig. 4a). Upon tilting or mild tapping of the sample vial, intense birefringence can be detected when viewed under

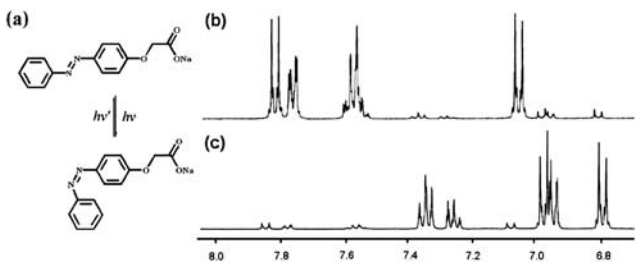


**Fig. 1** (a) The molecular structure of AzoNa. (b) and (c) $^1$H NMR spectra of AzoNa in $D_2O$ before and after UV light irradiation, respectively.

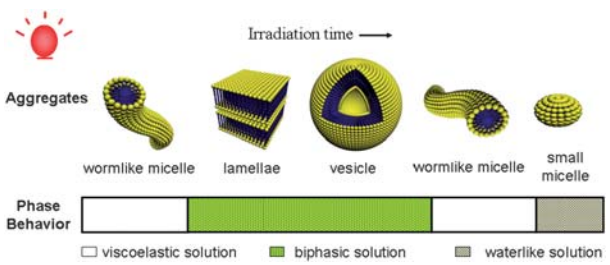


**Fig. 3** Structural evolution and phase behavior in the solution of 30 mM CTAB and 50 mM AzoNa varied with UV irradiation time.

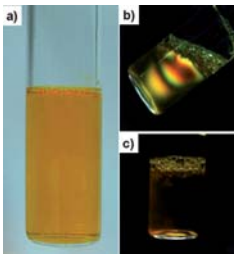


**Fig. 4** Macroscopic appearance of CTAB/AzoNa solution before UV irradiation (*state one*): (a) in the absence of polarizer; (b) tilted under polarizer; (c) rest under polarizer.

a crossed polarizer (Fig. 4b). On returning to the vertical position, the birefringence disappears again (Fig. 4c). Dynamic and steady rheology was further performed to investigate the flowing properties of this solution. As Fig. 5a shows, the sample exhibits typical rheological behavior of viscoelastic solution: at low oscillating frequency, the storage modulus G′ was dominant; while the loss modulus G″ was dominant at high frequency. Steady rheology indicates the sample exhibits shear-thinning behavior with a Newtonian plateau of around 80 PaS viscosity. Combined with the result of viscoelasticity and flow-birefringence, it is suggested that long flexible wormlike micelles in the CTAB/AzoNa solution. The entangled of wormlike micelle can be responsible for high viscoelasticity.[17] In a tilted state, the stress imposed deformation from gravity can cause alignment of wormlike micelle with the flow, which in turn leads to flow-birefringence. When shear is stopped, the worms rapidly revert to an isotropic state, and the birefringence disappears.[18]

When the sample was irradiated with 365 nm UV light for 0.5 h (donated as *state two*), the homogeneous solution separates into biphasic solution (see inset in Fig. 6). The upper phase has orange color with slightly bluish while the bottom phase is dark yellow. A strong birefringence can be detected under crossed polarizer (see inset in Fig. 6). Rheological measurement reveals the different flowing behavior of the upper and lower phase. As shown in Fig. 6, the upper phase is water-like with low viscosity while the lower phase exhibits shear-thinning behavior with a high viscosity.

FF-TEM, SAXS, and POM were further employed to explore the molecular self-assemblies. The FF-TEM image in Fig. 7a demonstrates the formation of global vesicles with 40–70 nm diameters in the upper phase, which is in coincide with rheological result. On the contrary, FF-TEM gives clear evidence of

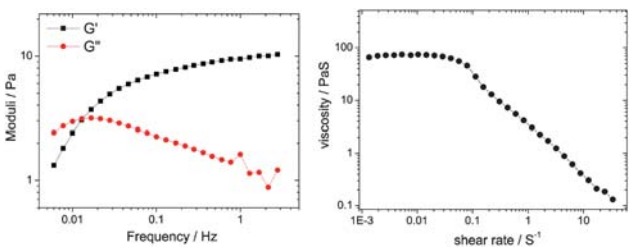


**Fig. 5** (a) Dynamic frequency sweep before UV irradiation showing strongly viscoelastic response; (b) steady shear property before UV irradiation with a Newtonian plateau and a shear-thinning behavior.

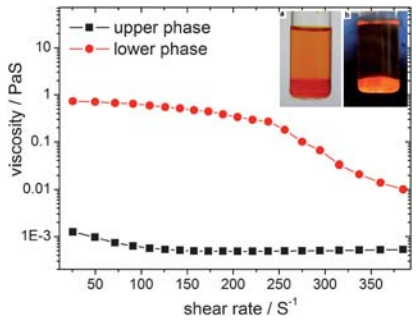


**Fig. 6** Steady rheology of CTAB/AzoNa exposed to UV light for 0.5 h (*state two*). The inset shows the macroscopic appearance of CTAB/AzoNa solution: (a) in the absence of polarizer; (b) in the presence of polarizer.

ordered lamellar structures in the lower phase (Fig. 7b), which is responsive for the high viscosity and strong birefringence. A typical Maltese crosses texture under POM was notable in the lower phase (Fig. 8a), confirming the existence of lamellar structures. Small Angle X-ray Scattering gives the quantitative description of molecular packing in the lamellar structures. As shown in Fig. 8b, a strong scattering signal ($q = 1.5$ nm$^{-1}$) could be found, which corresponds to a $d$-spacing of 4.2 nm and agrees well with double molecular length of CTAB (~2.1 nm). Hence, it is believed that CTAB adapts ordered tail-to-tail packing in the lamellar phase with AzoNa incorporating into surfactant headgroup (inset in Fig. 8b).

Further increasing UV irradiation time to 1.0 h results in a homogeneous viscous solution as shown in the inset of Fig. 9a (donated as *state three*). This solution shows evident

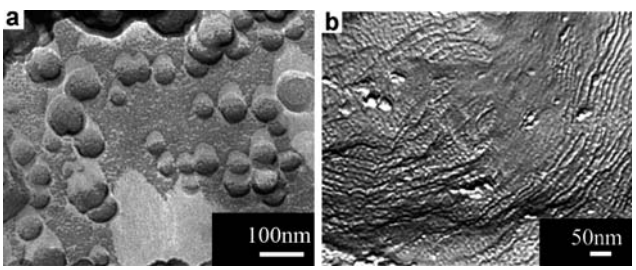


**Fig. 7** Freeze fracture-TEM image of CTAB/AzoNa after exposed to 365 nm UV light at *state two*: (a) upper phase; (b) lower phase.

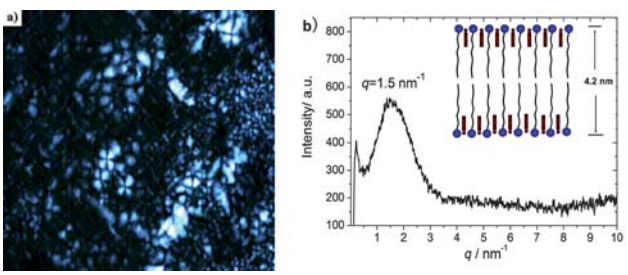


**Fig. 8** Lamellar phase of the lower phase in CTAB/AzoNa solution after exposed to 365 nm UV light at *state two*: (a) microscopy under polarizer (scale bar = 50 μm); (b) SAXS profile of the lamellar phase.

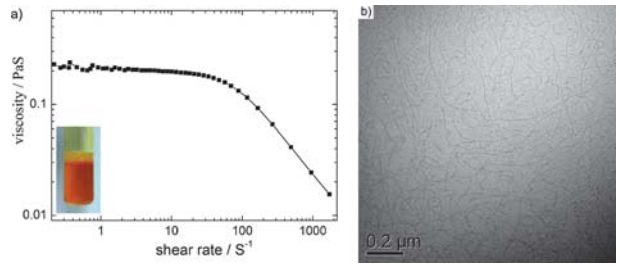


**Fig. 9** a) Steady shear of the CTAB/AzoNa solution after exposing to 365 nm UV light for 1.0 h (*state three*). The inset represents the appearance of the homogeneous solution. b) Cryo-TEM image of CTAB/AzoNa solution at *state three*.

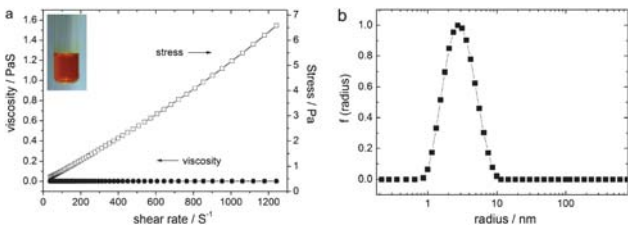


**Fig. 10** (a) Steady shear and (b) dynamic light scattering of CTAB/AzoNa solution after exposing to 365 nm UV light for 3.0 h (*state four*). The inset in Fig. 10a shows the macroscopic appearance of the homogeneous solution.

viscoelasticity, but not strong enough to be detected with dynamic oscillation experiment. Steady shear rheology in Fig. 9a shows shear-thinning behavior with a viscosity of 0.2 PaS. Under cross polarizer, no birefringence can be observed. The cryo-TEM image clearly demonstrated wormlike micelle formation in this viscoelastic solution (Fig. 9b). Dynamic light scattering reveals a slow mode that may correspond to structural relaxation of wormlike micelle network (Fig. S2).†

As the irradiation time increases to 3.0 h or longer (donated as *state four*), a homogeneous and dark yellow solution was obtained (see the inset in Fig. 10a). The steady shear result manifests a Newtonian fluid with low viscosity. Dynamic light scattering clearly demonstrates the existence of small aggregates with the hydrodynamic radius of approximate 3 nm (Fig. 10b), which is close to the extended length of CTAB molecule. Combined with the result of rheology and DLS, it is reasonable to believe that dispersed, small global micelle was formed at this state.

### Illustration of the multi-state and multi-scale self-assembled process

Hence, we have for the first time created a photo-modulated multi-state and multi-scale molecular self-assembled system in the pseudo cationic-anionic surfactant solution by virtue of binary-state molecular switch. At molecular level, the photo-active azobenzene unit can undergo trans/cis isomerization. At nanoscale level, distinct molecular architectures including long flexible wormlike micelle, global vesicle, ordered lamellar structure, and small global micelle, can be precisely regulated by a light signal. At macroscopic level, the sample can exhibit homogeneous viscoelastic solution with birefringence, biphasic solution, viscoelastic solution without birefringence, and water-like fluids. What happens to the surfactant solution and how does the light work?

It has been realized that molecular self-assemblies in the cationic-anionic surfactant systems mainly aroused from tight packing of oppositely charged surfactants, which is closely related to the stoichiometry and steric factor of cationic/anionic species. In the pseudo catanionic surfactant mixture of CTAB/AzoNa, although the concentration of both CTAB and AzoNa remains constant, the stoichiometry and steric factor in surfactant aggregates can be changed by light illumination. This is because, azobenzene can undergo photo-induced isomerism accompanied by large structural change as reflected in the dipole moment and change in geometry. The isomerization involves a decrease in the distance between the para carbon atoms in azobenzene from about 9.0 Å in the *trans*-form to 5.5 Å in the *cis*-form. Likewise, *trans*-azobenzene has no dipole moment while the dipole moment of the nonplanar *cis*-compound is 3.0 D.[10] It is believed that the difference in dipole moment can lead to the variation of hydrophobic/hydrophilic balance of azobenzene isomers. For example, in azobenzene-contained surfactants, the greater hydrophobicity of *trans*-surfactant gives it a lower critical micelle concentration.[19] Specifically, it is found that *trans*-AzoNa is highly hydrophobic with a solubility of 25 mM while light-triggered *cis*-AzoNa is more hydrophilic with a solubility of higher than 100 mM. Arising from electrostatic attraction and high hydrophobicity, *trans*-AzoNa can strongly intercalate into CTAB headgroup, which contributes to hydrophobic interaction and the screen of electrostatic repulsion.[20] In contrast, *cis*-AzoNa cannot effectively penetrate into surfactant aggregates as a consequence of hydrophilicity enhancement and fail to promote close packing of cationic-anionic species due to bulky steric limitation of *cis*-azobenzene.

Further experiments were conducted to confirm the above proposal. First, the aggregate-promoting ability of *trans*- and *cis*-AzoNa was distinguished by critical micelle concentration or CMC obtained from conductivity data (Fig. 11a), wherein the CMC value of CTAB/*trans*-AzoNa system (~0.055 mM) is notably lower than that of CTAB/*cis*-AzoNa system (~0.13 mM). So it is believed that *trans*-AzoNa can better promote surfactant aggregates. Second, the change in molecular packing of CTAB/AzoNa aggregates caused by photo-triggered *trans*/*cis* isomerization was clarified by steady florescence. Nile Red was chosen as the fluorescence probe because its excitation peak occurs at a long wavelength (575 nm) where absorption by the azobenzene group is minimal[21] and also because its emission is very environment-sensitive.[22] Nile Red fluorescence intensity is much greater in hydrophobic environments than in hydrophilic environment. Following excitation at 575 nm, the fluorescence emission spectrum was measured for each sample at different irradiation time. As shown in Fig. 11b, the initial solution gives strong Nile Red emission while continuing UV irradiation results in the decrease of fluorescence intensity. When UV irradiation time reaches 3.0 h, the Nile Red emission lowers to almost one eighth of the value before UV irradiation. Apparently, *trans*-AzoNa can lead to tight packing of cationic-anionic species while *cis*-AzoNa may cause loose molecular packing.

 

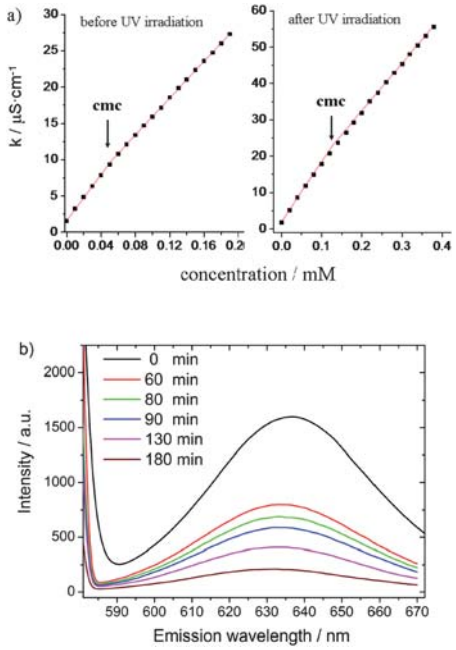


**Fig. 11** (a) Conductivity of CTAB/AzoNa (1 : 1 molar ratio) solution before and after UV irradiation; (b) Steady fluorescence of Nile Red in CTAB/AzoNa (30 mM/50 mM) as a function of UV irradiation time.

Combined with these results, we provide a possible scheme for the occurrence of photo-modulated multi-scale and multi-state molecular assemblies (Fig. 12). Before UV illumination (*state one*), *trans*-AzoNa can intercalate into the paraside layer of aggregates driven by electrostatic attraction and hydrophobic effect.[20] So the homogeneous visoelastic solution consisting of negatively charged wormlike micelle was attained, in which *trans*-AzoNa is in excess to CTAB. After further illumination of UV light (*state two*), a portion of the *trans*-AzoNa transformed into *cis*-AzoNa which is more hydrophilic and could not incorporate into surfactant aggregate. Consequently CTAB/*trans*-AzoNa mixture in the aggregates approaches the equimolar ratio and the aggregates charge was nearly neutralized, giving birth to biphasic surfactant solution consisting of bilayer vesicle and planar lamellae. In the lower phase, the *cis*-fraction of AzoNa is about 32% (the estimation of *cis*-AzoNa is described in the Supporting Information).† In the upper phase, the *cis*-fraction of AzoNa is slightly higher than that in the lower phase; however, the exact value cannot be obtained. After continuous UV light illumination, the concentration of *trans*-AzoNa in solution was further reduced and the amount of *trans*-AzoNa (~37%) is lower than that of CTAB, leading to the formation of positively charged cylindrical micelle and homogeneous solution (*state three*). When *trans*-AzoNa was mostly converted into *cis*-AzoNa (~83%), the electrostatic repulsive between CTAB headgroup becomes dominating factor that limits closely packing of surfactant molecule, resulting into positively charged global micelle (*state four*). The *zeta*-potential value at this stage (~3.0 mV) clarified the formation of positively charged micelle. In a word, the *trans*/*cis* molar ratio of AzoNa is responsible for the structural evolution of surfactant aggregates. In a complementary experiment, *state two* and *state three* can be created by mixing the solutions in *state one* and *state four* at the mixing proportions of 2 : 1 and 1 : 2, respectively.

To summarize, the photo-modulated multi-state molecular assemblies with distinct morphologies can be elegantly achieved *via* light stimulus. Meanwhile the photo-modulated multi-state molecular assemblies can be also amplified to solution properties at macroscopic scale. In addition, the photo-modulated self-assemblies can be reverted by exposing to visible light.

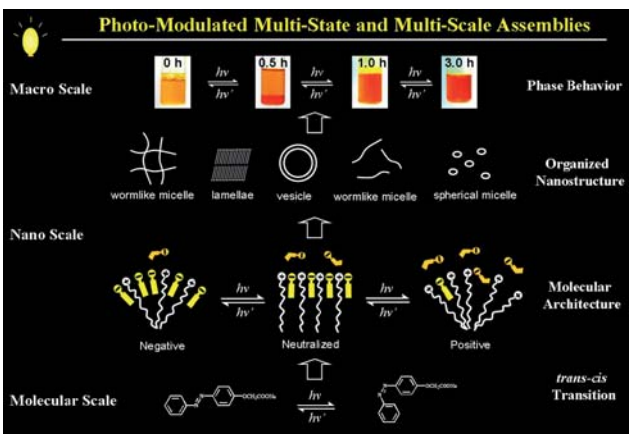


**Fig. 12** Representative scheme of photo-modulated multi-scale and multi-state self-assembled systems.

## Conclusions

In conclusion, we have for the first time designed a photo-modulated multi-state and multi-scale molecular self-assembled system by virtue of binary-state molecular switch. It is believed that the light-triggered *trans*/*cis* transition at molecular level can cause a large change in dipole moment and geometry of AzoNa, which influences the molecular packing of CTAB/AzoNa in the aggregates and leads to distinct molecular architectures and phase behavior. Depending on UV irradiation time, the self-assembled system can realize a four-state transition, i. e. long flexible wormlike micelle, global vesicle, planar lamellae, cylindrical micelle and small spherical micelle. It is anticipated that the concept of photo-modulated multi-state and multi-scale self-assembled system may be extended to the related research area such as molecular device, logic gates, and sensors.

## Acknowledgements

This work was supported by National Natural Science Foundation of China (20873001, 20633010, 50821061 and 20976003) and National Basic Research Program of China (Grant No. 2007CB936201).

## Reference

1 J.-M. Lehn, *Science*, 2002, **295**, 2400; S. Svenson, *Curr. Opin. Colloid Interface Sci.*, 2004, **9**, 201; J. H. Fuhrhop and W. Helfrich, *Chem. Rev.*, 1993, **93**, 1565; T. Shimizu, M. Masuda and H. Minamikawa, *Chem. Rev.*, 2005, **105**, 1401.
2 M. Johnsson, A. Wagenaar and J. B. F. N. Engberts, *J. Am. Chem. Soc.*, 2003, **125**, 757; Y. Y. Lin, X. Han, X. H. Cheng, J. B. Huang, D. H. Liang and C. L. Yu, *Langmuir*, 2008, **24**, 13918; K. Köhler, A. Meister, G. Förster, B. Dobner, S. Drescher, F. Ziethe,

W. Richter, F. Steiniger, M. Drechsler, G. Hause and A. Blume, *Soft Matter*, 2006, **2**, 77; H. Maeda, A. Yamamoto, H. Kawasaki, M. Souda, K. S. Hossain, N. Nemoto and M. Almgren, *J. Phys. Chem. B*, 2001, **105**, 5411; G. Verma, V. K. Aswal and P. Hassan, *Soft Matter*, 2009, **5**, 2919.

3 H. Sakai, Y. Orihara, H. Kodashima, A. Matsumura, T. Ohkubo, K. Tsuchiya and M. Abe, *J. Am. Chem. Soc.*, 2005, **127**, 13454; J. Y. Shin and N. L. Abbott, *Langmuir*, 1999, **15**, 4404; F. P. Hubbard Jr., G. Santonicola, E. W. Kaler and N. L. Abbott, *Langmuir*, 2005, **21**, 6131; F. P. Hubbard Jr. and N. L. Abbott, *Langmuir*, 2007, **23**, 4819; F. P. Hubbard Jr. and N. L. Abbott, *Soft Matter*, 2008, **4**, 2225; J. M. Kuiper and J. B. F. N. Engberts, *Langmuir*, 2004, **20**, 1152; L. Yang, N. Takisawa, T. Hayashita and K. Shirahama, *J. Phys. Chem.*, 1995, **99**, 8799; C. T. Lee, K. A. Smith and T. A. Hatton, *Macromolecules*, 2004, **37**, 5397; T. Shang, K. A. Smith and T. A. Hatton, *Langmuir*, 2003, **19**, 10764; T. Shang, K. A. Smith and T. A. Hatton, *Langmuir*, 2006, **22**, 1436; K. Murata, M. Aoki, T. Suzuki, T. Harada, H. Kawabata, T. Komri, F. Ohseto, K. Ueda and S. Shinkai, *J. Am. Chem. Soc.*, 1994, **116**, 6664; A. Vesperinas, J. Eastoe, P. Wyatt, I. Grillo, R. K. Heenan, J. M. Richards and G. A. Bell, *J. Am. Chem. Soc.*, 2006, **128**, 1468; J. Eastoe, P. Wyatt, M. Sanchez-Dominguez, A. Vesperinas, A. Paul, R. Heenan and I. Grillo, *Chem. Commun.*, 2005, 2785; R. F. Tabor, R. J. Oakley, J. Eastoe, C. F. J. Faul, I. Grillo and R. Heenan, *Soft Matter*, 2009, **5**, 78; Y. P. Wang, N. Ma, Z. Q. Wang and X. Zhang, *Angew. Chem., Int. Ed.*, 2007, **46**, 2823; R. Kumar and S. R. Raghavan, *Soft Matter*, 2009, **5**, 797.

4 T. S. Davies, A. M. Ketner and S. R. Raghavan, *J. Am. Chem. Soc.*, 2006, **128**, 6669; H. Q. Yin, Z. K. Zhou, J. B. Huang, R. Zheng and Y. Y. Zhang, *Angew. Chem., Int. Ed.*, 2003, **42**, 2188; S. R. Raghavan, H. Edlund and E. W. Kaler, *Langmuir*, 2002, **18**, 1056; P. R. Majhi and A. Blume, *J. Phys. Chem. B*, 2002, **106**, 10753; Y. Y. Lin, Y. Qiao, Y. Yan and J. B. Huang, *Soft Matter*, 2009, **5**, 3047.

5 Y. Kakizawa, H. Sakai, A. Yamaguchi, Y. Kondo, N. Yoshino and M. Abe, *Langmuir*, 2001, **17**, 8044; K. Tsuchiya, Y. Orihara, Y. Kondo, N. Yoshino, T. Ohkubo, H. Sakai and M. Abe, *J. Am. Chem. Soc.*, 2004, **126**, 12282; B. S. Gallardo, K. L. Metcalfe and N. L. Abbott, *Langmuir*, 1996, **12**, 4116.

6 L. I. Jong and N. L. Abbott, *Langmuir*, 1998, **14**, 2235; N. K. P. Samuel, M. Singh, K. Yamaguchi and S. L. Regen, *J. Am. Chem. Soc.*, 1985, **107**, 42; S. Ghosh, K. Irvin and S. Thayumanavan, *Langmuir*, 2007, **23**, 7916.

7 J. M. J. Paulusse and R. P. Sijbesma, *Angew. Chem., Int. Ed.*, 2004, **43**, 4460; T. Naota and H. Koori, *J. Am. Chem. Soc.*, 2005, **127**, 9324.

8 R. Oda, I. Huc and S. J. Candau, *Angew. Chem., Int. Ed.*, 1998, **37**, 2689; J. C. Hao, J. Z. Wang, W. M. Liu, R. Abdel-Rahem and H. Hoffmann, *J. Phys. Chem. B*, 2004, **108**, 1168; Y. Yan, W. Xiong, X. S. Li, T. Lu, J. B. Huang, Z. C. Li and H. L. Fu, *J. Phys. Chem. B*, 2007, **111**, 2225.

9 I. Willner and S. Rubin, *Angew. Chem., Int. Ed. Engl.*, 1996, **35**, 367; G. Feher, J. P. Allen, M. Okamura and D. C. Rees, *Nature*, 1989, **339**, 111; L. Stryer, *Annu. Rev. Neurosci.*, 1986, **9**, 87.

10 G. S. Kumar and D. C. Neckers, *Chem. Rev.*, 1989, **89**, 1915; C. Dugave and L. Demange, *Chem. Rev.*, 2003, **103**, 2475.

11 P. H. Rasmussen, P. S. Ramanujam, S. Hvilsted and R. H. Berg, *J. Am. Chem. Soc.*, 1999, **121**, 4738; T. Ikeda and O. Tsutsumi, *Science*, 1995, **268**, 1873; V. Ferri, M. Elbing, G. Pace, M. D. Dickey, M. Zharnikov, P. Samor, M. Mayor and M. A. Rampi, *Angew. Chem., Int. Ed.*, 2008, **47**, 3407.

12 H. Sakai, A. Matsumura, S. Yokoyama, T. Saji and M. Abe, *J. Phys. Chem. B*, 1999, **103**, 10737.

13 X. D. Song, J. Perlstein and D. G. Whitten, *J. Am. Chem. Soc.*, 1997, **119**, 9144.

14 A. M. Ketner, R. Kumar, T. S. Davies, P. W. Elder and R. S. Raghavan, *J. Am. Chem. Soc.*, 2007, **129**, 1553.

15 J. Eastoe, A. H. Zou, Y. Espidel, O. Glatter and I. Grillo, *Soft Matter*, 2008, **4**, 1215.

16 E. W. Kaler, K. L. Herrrington, A. K. Murthy and J. A. Zasadzinski, *J. Phys. Chem.*, 1992, **96**, 6698; J.-B. Huang and G.-X. Zhao, *Colloid Polym. Sci.*, 1995, **273**, 156; P. K. Yuet and D. Blankschtein, *Langmuir*, 1996, **12**, 3802; A. J. O'Connor, T. A. Hatton and A. Bose, *Langmuir*, 1997, **13**, 6931; H. T. Jung, B. Coldren, J. A. Zasadzinski, D. J. Iampietro and E. W. Kaler, *Proc. Natl. Acad. Sci. U. S. A.*, 2001, **98**, 1353; J. C. Hao and H. Hoffmann, *Curr. Opin. Colloid Interface Sci.*, 2004, **9**, 279; E. F. Marques, O. Regev, A. Khan and B. Lindman, *Adv. Colloid Interface Sci.*, 2003, **100**, 83; Y. Xia, I. Goldmints, P. W. Johnson, T. A. Hatton and A. Bose, *Langmuir*, 2002, **18**, 3822.

17 S. J. Candau, E. Hirsch and R. Zana, *J. Colloid Interface Sci.*, 1985, **105**, 521; M. E. Cates and S. J. Candau, *J. Phys.: Condens. Matter*, 1990, **2**, 6869; S. J. Candau, A. Khatory, F. Lequeux and F. Kern, *J. Phys. IV*, 1993, **3**, 197; L. J. Magid, *J. Phys. Chem. B*, 1998, **102**, 4064; Y. I. Gonzalez and E. W. Kaler, *Curr. Opin. Colloid Interface Sci.*, 2005, **10**, 256; C. A. Dreiss, *Soft Matter*, 2007, **3**, 956; H. Rehage and H. Hoffmann, *Mol. Phys.*, 1991, **74**, 933.

18 B. D. Frounfelker, G. C. Kalur, B. H. Cipriano, D. Danino and S. R. Raghavan, *Langmuir*, 2009, **25**, 167; T. Shikata, S. J. Dahman and D. S. Pearson, *Langmuir*, 1994, **10**, 3470; B. A. Schubert, E. W. Kaler and N. J. Wagner, *Langmuir*, 2003, **19**, 4079.

19 T. Hayashita, T. Kurosawa, T. Miyata, K. Tanaka and M. Igawa, *Colloid Polym. Sci.*, 1994, **272**, 1611; C. T. Lee, K. A. Smith and T. A. Hatton, *Macromolecules*, 2004, **37**, 5397.

20 P. J. Kreke, L. J. Magid and J. C. Gee, *Langmuir*, 1996, **12**, 699; S. Mohanty, H. T. Davis and A. V. McCormick, *Langmuir*, 2001, **17**, 7160; M. Vermathen, P. Stiles, S. J. Bachofer and U. Simonis, *Langmuir*, 2002, **18**, 1030.

21 B. A. Cicciarelli, T. A. Hatton and K. A. Smith, *Langmuir*, 2007, **23**, 4753.

22 D. L. Sackett and J. Wolff, *Anal. Biochem.*, 1987, **167**, 228; M. C. A. Stuart, J. C. van de Pas and J. B. F. N. Engberts, *J. Phys. Org. Chem.*, 2005, **18**, 929.

 